Online ISSN 1848-3380, Print ISSN 0005-1144
ATKAFF 54(3), 348–355(2013)

Czeslaw T. Kowalski, Robert Wierzbicki, Marcin Wolkiewicz

Stator and Rotor Faults Monitoring of the Inverter-Fed Induction Motor Drive using State Estimators

DOI 10.7305/automatika.54-3.167
UDK 681.5.09.015.44.03:621.313.33-253-226.1
IFAC 2.1.4; 1.1

Original scientific paper

The paper deals with the application of the Extended Kalman Filter and the Extended Luenberger Observer algorithms for the stator and rotor fault detection of the induction motor fed by PWM inverter. The induction motor conditions are analyzed using estimated rotor and stator-winding resistance. Mathematical models of the extended state estimators are presented, in which the stator and rotor resistances are added as additional electromagnetic state variables. Experimental results for the inverter-fed induction motor, with shorted stator-turns and broken rotor bars, are presented and analysed.

Key words: induction machines, diagnostics, fault detection, Kalman filter, Luenberger observer

Nadgledanje statorskih i rotorskih pogrešaka asinkronog motora napajanog inverterom koristeći estimatore stanja. Ovaj radi proučava primjenu algoritama proširenog Kalmanovog filtra i proširenog Luenbergerovog observera za detekciju pogreške statora i rotora asinkronog motora napajanog PWM inverterom. Stanja asinkronog motora analizirana su korištenjem estimiranog otpora statorskih i rotorskih namota. Prikazani su matematički modeli proširenih estimatora stanja u kojima su otpori statora i rotora dodani kao dodatne varijable stanja. Prikazani su i analizirani eksperimentalni rezultati za asinkroni motor napajan inverterom s kratko spojenim statorskim namotima i prekinutim rotoskim polugama.

Ključne riječi: asinkroni stroj, dijagnostika, detekcija pogreške, Kalmanov filtar, Luenbergerov observer

1 INTRODUCTION

Induction motor (IM) drives are widely used nowadays in many industrial processes and thus problems of their maintenance and fault detection become more important. The failure of the motor can cause substantial financial losses and even damage of the whole drive system. Needs of the analysis of an actual technical condition of IMs caused in the last years the great development of diagnostic methods and techniques, which could be used in the fault detection of IMs drives [1], [2].

Stator and rotor faults are responsible respectively for 37% and 13% of the IM failures and, after the bearing faults, are the most frequent reasons of the IM damages. In monitoring and diagnosis of IM drives mostly the stator current and mechanical vibrations are used as diagnostic signals.

Due to simplicity of measurements, the stator current signals are more widely used for this purpose and thus different analysis methods have been developed, based on detection of sidebands harmonics at certain frequencies. Such methods like Fast Fourier Transform (FFT), Short Time Fourier Transform (STFT), the Wavelet Transform (WT) and the high order transformation (HOT) are more and more often applied [1]-[3].

In the case of IMs supplied from frequency inverters such analysis is much more complicated due to additional harmonics generated by the inverter supply, which overlaps with harmonics caused by the stator or rotor faults. Therefore, the usual techniques, based on spectral analysis of the stator current signal are not well adapted in adjustable speed motor drives and some authors have proposed the methods based on an on-line estimation of motor parameters changes due to motor failures [4]. In normal operation conditions, estimated parameters have nominal values, which change in the limited range (due to a temperature rise). If the motor fault occurs, these changes are growing or decreasing much faster, so the analysis of the estimated parameter changes enables the detection of the failure.

In this paper, the diagnostic technique of the stator and rotor faults of the inverter-supplied IM by on-line parameter identification is presented, using the Extended Kalman Filter algorithm (EKF) and Extended Luenberger Observer

(ELO). Analysis of the changes of the estimated rotor and stator resistances is used for fault detection of the PWM inverter-fed IM. The main goal of this paper is to show the practical digital realization the EKF and ELO algorithms in the fault detection task of the IM and to prove the earlier theoretical results presented in [5].

2 MATHEMATICAL MODEL OF THE INDUCTION MOTOR

Using well-known simplifying assumptions, the IM mathematical model can be described by the space vector equations in the stationary ($\alpha - \beta$) reference frame as in [5, 6].

– the state equation:

$$\dot{x}(t) = A(\omega_m) \cdot x(t) + B \cdot u(t) \tag{1}$$

– the output equation:

$$y(t) = C \cdot x(t) \tag{2}$$

where:

– the state vector (of electromagnetic state variables):

$$x(t) = \left[\begin{array}{cccc} i_{s\alpha} & i_{s\beta} & \psi_{r\alpha} & \psi_{r\beta} \end{array} \right]^T \tag{3}$$

– the input and output vectors:

$$u(t) = \left[\begin{array}{cc} u_{s\alpha} & u_{s\beta} \end{array} \right]^T \tag{4}$$

$$y(t) = \left[\begin{array}{cc} i_{s\alpha} & i_{s\beta} \end{array} \right]^T \tag{5}$$

– the state matrix:

$$A(\omega_m) = \left[\begin{array}{cccc} a & 0 & b & c \\ 0 & a & -c & b \\ d & 0 & -e & -\omega_m \Omega_b \\ 0 & d & \omega_m \Omega_b & -e \end{array} \right] \tag{6}$$

– the input **B** and output **C** matrices:

$$B = \left[\begin{array}{cccc} \frac{\Omega_b}{\sigma \cdot x_s} & 0 & 0 & 0 \\ 0 & \frac{\Omega_b}{\sigma \cdot x_s} & 0 & 0 \end{array} \right]^T \tag{7}$$

$$C = \left[\begin{array}{cccc} 1 & 0 & 0 & 0 \\ 0 & 1 & 0 & 0 \end{array} \right] \tag{8}$$

where:

$$a = -\frac{1}{x_s \sigma} r_s \Omega_b - \frac{1-\sigma}{x_r \sigma} r_r \Omega_b, b = \frac{k_r r_r \Omega_b}{x_r x_s \sigma}$$

$$c = \frac{\omega_m k_r \Omega_b}{x_s \sigma}, d = \frac{x_M}{x_r} r_r \Omega_b, e = \frac{r_r \Omega_b}{x_r}, k_r = \frac{x_M}{x_r}$$

and: $u_{s\alpha}$, $u_{s\beta}$, $i_{s\alpha}$, $i_{s\beta}$, $\psi_{s\alpha}$, $\psi_{s\beta}$ - coordinates of the stator voltage and current vector, and the rotor flux vector, respectively, r_s, r_r, x_s, x_r, x_M -stator and rotor resistances, stator and rotor reactances, mutual reactance, respectively, σ - total leakage coefficient, ω_m - rotor speed, Ω_b - reference angular pulsation.

3 EXTENDED KALMAN FILTER ALGORITHM

In According to the Kalman filter theory [7], IM model (1)-(8), must be written in the discrete form:

$$\begin{aligned} x_R(k+1) &= A_R(k)x_R(k) + B_R(k)u_R(k) + w(k) \\ y_R(k) &= C_R(k)x_R(k) + v(k) \end{aligned} \tag{9}$$

where w and v are matrices of the process and measurement noises, and matrices $\mathbf{A}_R$, $\mathbf{B}_R$, $\mathbf{C}_R$ and vector $\mathbf{u}_R$ are filled respectively with zeros in last rows or columns comparing to (6)-(8) and (4).

Estimation of state vector is realized in the following steps:

- **step 1** - the state vector predictor $\hat{\mathbf{x}}_R(k+1)$ in the step *(k+1)* is calculated using input $\mathbf{u}(k)$ and state vector predictor in the previous step $\hat{\mathbf{x}}_R(k)$:

$$\hat{x}_R(k+1/k) = A_R(\omega_m(k)) \cdot \hat{x}_R(k/k) + B_R \cdot u(k) \tag{10}$$

- **step 2** - the covariance matrix of the prediction error is estimated:

$$P(k+1/k) = F_{\mathrm{R}}(k)P(k)F_{\mathrm{R}}(k)^T + Q(k) \tag{11}$$

where $\mathbf{F}_R(k) = \frac{\partial f(x_R(k/k),u(k),k)}{\partial x_R(k/k)}|_{x_R=\hat{x}_R(k/k)}$,

Q - the state noise covariance matrix,

- **step 3** - the Kalman filter gain matrix is calculated using following equations:

$$\begin{aligned} K(k+1) = P(k+1/k) \cdot C_R(k+1)^T \cdot \\ \cdot [C_R(k+1) \cdot P(k+1/k) \cdot C_R(k+1) + R]^{-1} \end{aligned} \tag{12}$$

where $\mathbf{R}$ - the output (measurement) noise covariance matrix,

- **step 4** - the correction of the state vector estimate (according to the general form of Kalman filter model) is calculated:

$$\begin{aligned} \hat{x}_R(k+1/k+1) = \hat{x}_R(k+1/k) + K(k+1) \cdot \\ \cdot [y(k+1) - C_R(k+1) \cdot \hat{x}_R(k+1/k)] \end{aligned} \tag{13}$$

- **step 5** - the filter covariance matrix of the state estimation error is updated:

$$P(k+1/k+1) = [I - K(k+1) \cdot C_R(k+1)] \cdot \cdot P(k+1/k) \quad (14)$$

- **step 6** - return to the first step.

The convergence and dynamical behavior of the Kalman filter algorithm depends strongly on the suitable chosen covariance matrices $\mathbf{Q}$ and $\mathbf{R}$ [5].

Stator and rotor resistance are selected as additional state variables, so two new extended state vectors for stator and rotor fault diagnosis are defined as follows:

$$x_R^s(t) = \left[\begin{array}{ccccc} i_{s\alpha} & i_{s\beta} & \psi_{r\alpha} & \psi_{r\beta} & r_s \end{array} \right]^T \quad (15)$$

$$x_R^r(t) = \left[\begin{array}{ccccc} i_{s\alpha} & i_{s\beta} & \psi_{s\alpha} & \psi_{s\beta} & r_r \end{array} \right]^T \quad (16)$$

where: $\psi_{s\alpha}$, $\psi_{s\beta}$ - components of the stator flux vector, calculated based on the well-known algebraic equations, using stator current and rotor flux vector components.

4 EXTENEDED LUENBERGER OBSERVER ALGORITHM

4.1 Rotor resistance estimation

For the estimation of the rotor winding resistance, the state vector (3) of the mathematical model (1)-(8) has been extended with this parameter as follows:

$$\hat{x}_R^r = \left[\begin{array}{ccccc} \hat{i}_{s\alpha} & \hat{i}_{s\beta} & \hat{\psi}_{r\alpha} & \hat{\psi}_{r\beta} & \hat{r}_r \end{array} \right]^T. \quad (17)$$

According to the Luenberger theory [7], [8] the extended full-order state observer can be developed in the form:

$$\frac{d\hat{x}_R^r}{dt} = \hat{A}_R^r(\hat{x}_R^r)\,\hat{x}_R^r + B_R u + G_R^r(\hat{i}_s - i_s) \quad (18)$$

where the input vector as in (4), and:

- the extended state matrix as in (19):,

$$\hat{A}_R^r(\hat{r}_r, \omega_m) = \left[\begin{array}{ccccc} -\left(\frac{1}{x_s\sigma} r_s \Omega_b + \frac{1-\sigma}{x_r\sigma}\hat{r}_r\Omega_b\right) & 0 & \frac{k_r\hat{r}_r\Omega_b}{x_r x_s\sigma} & \frac{\omega_m k_r \Omega_b}{x_s\sigma} & 0 \\ 0 & -\left(\frac{1}{x_s\sigma} r_s \Omega_b + \frac{1-\sigma}{x_r\sigma}\hat{r}_r\Omega_b\right) & -\frac{\omega_m k_r \Omega_b}{x_s\sigma} & \frac{k_r\hat{r}_r\Omega_b}{x_r x_s\sigma} & 0 \\ \frac{x_m}{x_r}\hat{r}_r\Omega_b & 0 & -\frac{\hat{r}_r\Omega_b}{x_r} & -\omega_m\Omega_b & 0 \\ 0 & \frac{x_m}{x_r}\hat{r}_r\Omega_b & \omega_m\Omega_b & -\frac{\hat{r}_r\Omega_b}{x_r} & 0 \\ 0 & 0 & 0 & 0 & 0 \end{array} \right] \quad (19)$$

- the extended input matrix:

$$B_R = \left[\begin{array}{ccccc} \frac{\Omega_b}{\sigma \cdot x_s} & 0 & 0 & 0 & 0 \\ 0 & \frac{\Omega_b}{\sigma \cdot x_s} & 0 & 0 & 0 \end{array} \right]^T \quad (20)$$

- the extended observer gain matrix:

$$G_R^r = \left[\begin{array}{cccccc} g_1 & g_2 & g_3 & g_4 & k_{or}\left(\hat{\psi}_{r\alpha} - x_m\hat{i}_{s\alpha}\right) \\ -g_2 & g_1 & -g_4 & g_3 & k_{or}\left(\hat{\psi}_{r\beta} - x_m\hat{i}_{s\beta}\right) \end{array} \right]^T \quad (21)$$

where:

$$g_1 = -(k_o - 1)\left(\frac{r_s}{\sigma x_s} + \frac{1}{\sigma T_r}\right),$$
$$g_2 = (k_o - 1)\omega_m, g_4 = -c(k_o - 1)\omega_m,$$
$$g_3 = (k_o^2 - 1)\left(-c\left(\frac{r_s}{\sigma x_s} + \frac{1-\sigma}{\sigma T_r}\right) + \frac{x_m}{T_r}\right) + + c(k_o - 1)\left(\frac{r_s}{\sigma x_s} + \frac{1}{\sigma T_r}\right)$$

$\hat{r}_r$ - estimated rotor resistance in the previous numerical step, k_o, k_{or} - positive constants.

4.2 Stator resistance estimation

For the estimation of the stator winding resistance, the state vector of the mathematical model (1)-(8) has been extended with this parameter as follows:

$$\hat{x}_R^s = \left[\begin{array}{cccccc} \hat{i}_{s\alpha} & \hat{i}_{s\beta} & \hat{\psi}_{r\alpha} & \hat{\psi}_{r\beta} & \hat{r}_s \end{array} \right]^T \tag{22}$$

Thus the extended full-order state observer can be developed in the form:

$$\frac{d\hat{x}_R^s}{dt} = \hat{A}_R^s\left(\hat{x}_R^s\right)\hat{x}_R^s + B_R u + G_R^s(\hat{i}_s - i_s) \tag{23}$$

where the input vector as in (4), and the extended state matrix $\mathbf{B_R}$ as (19),

- the extended observer gain matrix:

$$G_R^s = \left[\begin{array}{ccccc} g_1 & g_2 & g_3 & g_4 & k_{os}\hat{i}_{s\alpha} \\ -g_2 & g_1 & -g_4 & g_3 & k_{os}\hat{i}_{s\beta} \end{array} \right]^T \tag{24}$$

where: $\hat{r}_s$ - estimated stator resistance calculated in the previous numerical step,
k_{os} - positive constant,

- the extended state matrix:

$$\hat{A}_R^s(\hat{r}_s,\omega_m) = \left[\begin{array}{cccc} -\left(\frac{1}{x_s\sigma}\hat{r}_s\Omega_b + \frac{1-\sigma}{x_r\sigma}r_r\Omega_b\right) & 0 & \frac{k_r r_r \Omega_b}{x_r x_s \sigma} & \frac{\omega_m k_r \Omega_b}{x_s\sigma} & 0 \\ 0 & -\left(\frac{1}{x_s\sigma}\hat{r}_s\Omega_b + \frac{1-\sigma}{x_r\sigma}r_r\Omega_b\right) & -\frac{\omega_m k_r \Omega_b}{x_s\sigma} & \frac{k_r r_r \Omega_b}{x_r x_s \sigma} & 0 \\ \frac{x_m}{x_r}r_r\Omega_b & 0 & -\frac{r_r\Omega_b}{x_r} & -\omega_m\Omega_b & 0 \\ 0 & \frac{x_m}{x_r}r_r\Omega_b & \omega_m\Omega_b & -\frac{r_r\Omega_b}{x_r} & 0 \\ 0 & 0 & 0 & 0 & 0 \end{array} \right] \tag{25}$$

5 EXPERIMENTAL RESULTS FOR ROTOR AND STATOR FAULTS

5.1 General description of experimental benchmark

In order to check the theoretical backgrounds and the possibilities of the EKF and ELO application for the on-line detection of stator and rotor fault of IM, experimental tests were performed in the Direct Field Oriented (DFOC) structure, presented in Fig. 1a.

Laboratory tests were realized in the laboratory set-up, for the 1.5kW IM with a few specially prepared rotors and a stator winding. Tested motor has 412 turns per stator phase-winding and 28 bars in rotor. In experimental tests different winding failures were modeled physically (with exchangeable rotors having different numbers of damaged bars: health and from 1 to 8 broken rotor bars, as well as for different number of shorted turns in the stator winding: 1, 2, 4, 8, 10, and 16).

The IM was supplied from the frequency converter, with Space Vector Modulator. The vector control structure DFOC, together with the EKF or ELO and residuum determination were realized using digital signal processor DS1104 of dSPACE. The whole application has been written in C language. The general scheme of the laboratory set-up is given in Fig. 1b.

5.2 Rotor fault detection

The examples of the experimental drive system operation with on-line estimation of rotor winding resistance using EKF and ELO are demonstrated in Fig. 2 and Fig. 3, for speed reference and load torque changes, respectively.

In Fig. 2, on the left hand side the transients for healthy motor are presented, and on the right hand side the similar transients for the motor with 7 broken rotor bars are

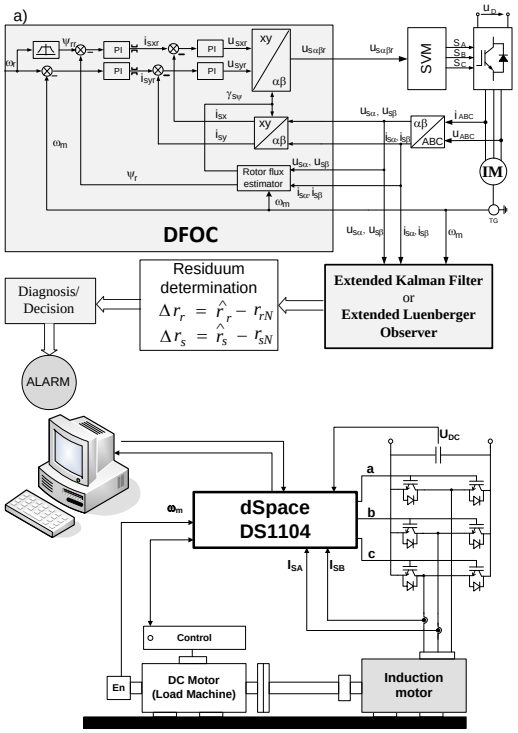

Fig. 1. Schematic diagrams of the experimental benchmark: a) structure of the DFOC drive system with on-line diagnosis of winding faults; b) laboratory set-up

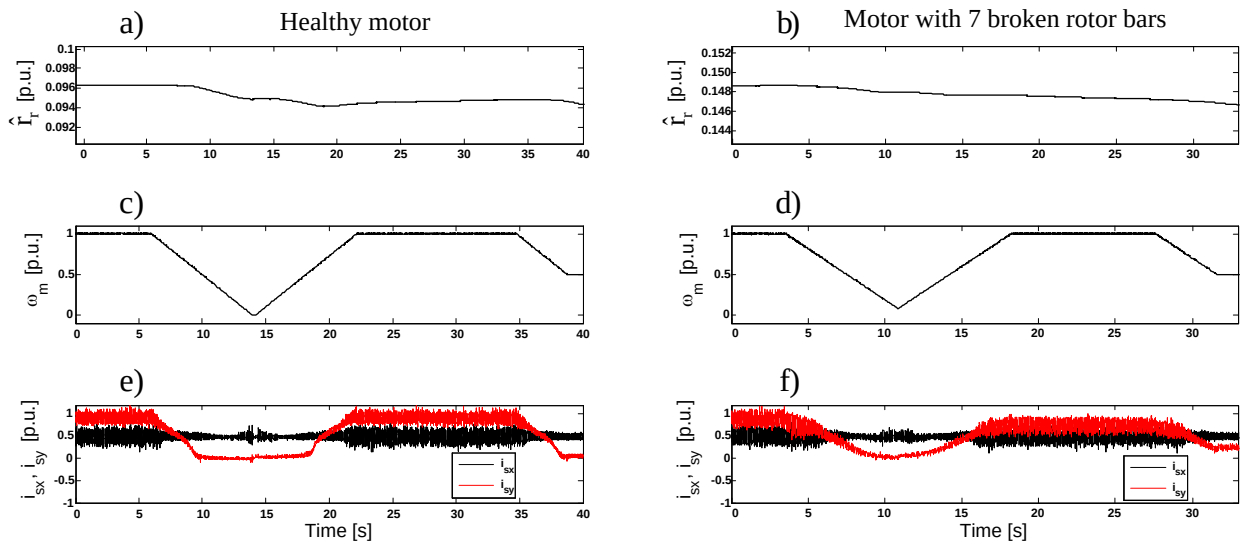

Fig. 2. Experimental transients of estimated rotor resistance under changes of reference speed: estimated rotor resistance (a,b), motor speed (c,d) and stator current vector components x-y (e,f) for the EKF used as state estimator

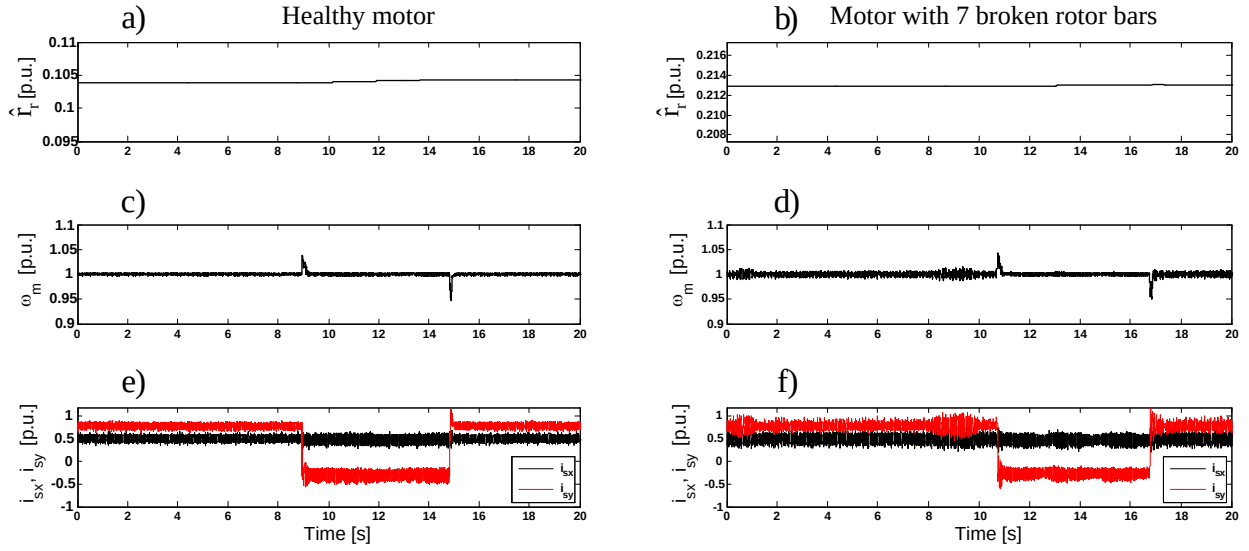

Fig. 3. Experimental transients of estimated rotor resistance under load torque changes: estimated rotor resistance (a,b), motor speed (c,d) and stator current vector components x-y (e,f) for the ELO used as state estimator Stator fault detection

shown, when EKF was used. The reference speed has been changed slowly from nominal to zero value and vice versa, and next from nominal to 50%, as can be seen in Fig. 2b. Change of the rotor speed in such a wide range causes very small changes of the rotor resistance, which have no influence on the fault detection of the rotor. As can be seen, estimated rotor resistance reaches much bigger values in a case of faulted rotor (Fig. 2b) than for healthy rotor case (Fig. 2a). Similar results can be obtained when ELO is used for rotor resistance estimation.

In Fig. 3 the changes of estimated rotor resistance under constant speed and changeable load torque are demonstrated, when ELO was used. The driven motor is nominally loaded, except of the time period t = (9÷15)s, when load torque is switched-off. Similarly, as for EKF based fault detector, ELO algorithm is not sensitive to step

changes of the load torque and estimates the rotor resistance properly as well for healthy (Fig. 3a,c,e) as for the faulted motor (Fig. 3b,d,f). The estimated rotor resistance for the faulted rotor case (Fig. 3b) is much bigger than for the healthy rotor (Fig. 3a), similarly as for the EKF detector.

5.3 Stator fault detection

The experimental tests were done for the healthy motor and for the motor with different number of shorted turns in the one phase of the stator winding. In the following figures examples of results obtained for the EKF and next for the ELO are presented. These both fault detectors operate independently on the vector control structure and are responsible only for the reconstruction of the stator or rotor resistance changes.

In Fig. 4 and Fig. 5 the results of the stator resistance estimation using EKF are demonstrated, in case of 16 shorted turns of the stator winding, for nominal load torque and nominal reference speed values. The fault was "activated" by realization of 16 short circuit turns in the real motor at the time t=75s, and "removed" at the time t=145s.

It can be seen that for the stator winding fault (16 shorted turns, which is around 4 % of total turns number), the stator winding resistance decreases over 30%. The range of the stator resistance changes due to the turns' short circuit is much smaller in the closed loop drive system than in open-loop (e.g. *U/f*=const strategy) [5]. However it should be noticed, that the sensitivity of the EKF based method is from 6 shorted turns. Moreover, the stator resistance estimation using EKF requires long computation time (6-7s), what is not suitable for the stator fault detection, as so long "decision time" can cause the permanent damage of the stator winding due to an avalanche character of this fault.

The similar tests were realized for the ELO used as the stator resistance estimator under healthy and faulted condition of the IM operating in the close-loop vector structure.

In Fig. 6 and Fig. 7 exemplary results of such tests are presented, for different number of shorted stator winding turns, for nominal load torque and reference speed. The conducted tests prove that in a case of ELO the on-line detection of the stator fault is possible even for a single shorted turn, which is big advantage of the proposed approach, in contrary to the EKF application.

The fault indicator is proposed for the evaluation of fault detection effectiveness. In a case of the rotor and stator damage this indicator takes the following forms, respectively:

$$\delta r_r = \frac{\hat{r}_r - r_{rN}}{r_{rN}} 100\% \tag{26}$$

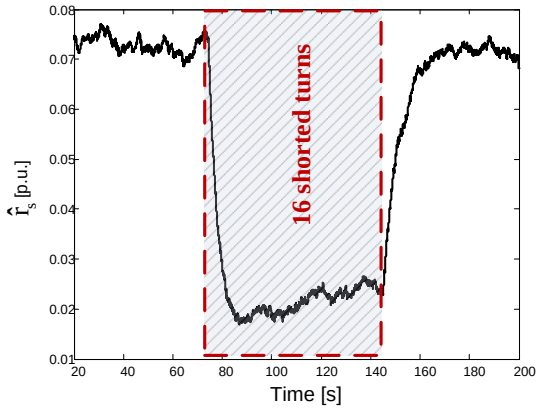

Fig. 4. Experimental transients of the estimated stator resistance using EKF in a case of 16 shorted turns, for nominal torque and reference speed $\omega_{mz} = 1$ [p. u.]

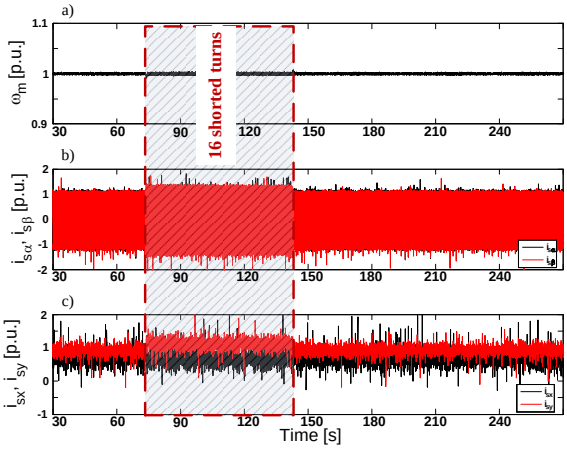

Fig. 5. Experimental transients of the motor speed (a) and components of the stator current vector in a case of 16 shorted turns, for nominal torque and reference speed $\omega_{mr} = 1$ [p. u.] (EKF)

$$\delta r_s = \left| \frac{\hat{r}_s - r_{sN}}{r_{sN}} \right| 100\% \tag{27}$$

where r_{sN}, r_{rN} - nominal values of stator and rotor resistances.

Comparison of the results obtained for EKF and ELO, in a case of rotor fault detection, is shown in Fig. 8.

The percentage rotor fault indicator increases with the increasing fault level for both tested estimation algorithms. It should be noticed that this indicator takes little bigger values for ELO than for EKF, starting from 5 broken rotor

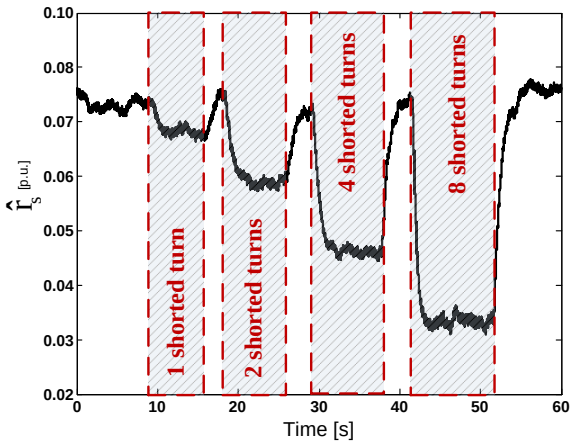

Fig. 6. Experimental transients of the estimated stator resistance using ELO in a case of different number of shorted turns, for nominal torque and reference speed ω_{mz}=1 [p.u.]

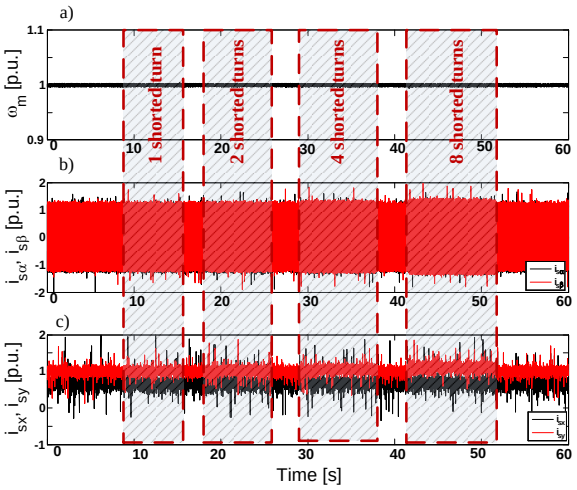

Fig. 7. Experimental transients of the motor speed (a) and components of the stator current vector in a case of different number of shorted turns, for nominal torque and reference speed $\omega_{mz} = 1$ [p. u.] (ELO)

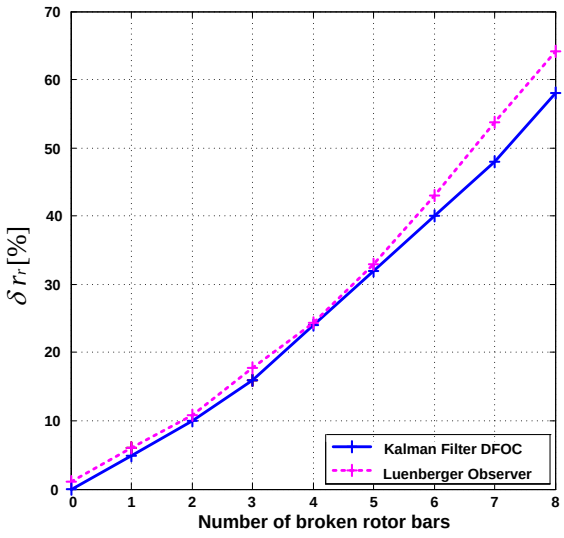

Fig. 8. The rotor fault indicator versus number of broken rotor bars

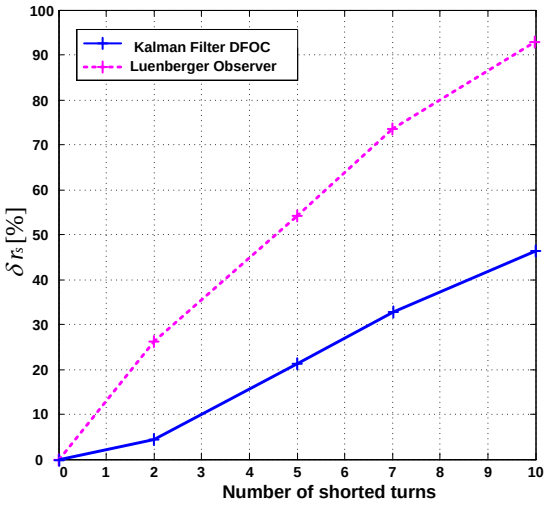

Fig. 9. The stator fault indicator versus number of shorten turns of stator winding

bars. Thus it can be said that both estimators, EKF and ELO indicate the rotor fault level with similar accuracy.

Comparison of the results obtained for EKF and ELO in a case of stator fault detection is presented in Fig. 9.

For the stator winding failure the proposed percentage fault indicator (27) increases with the increasing fault level for both tested estimation algorithms. Lower sensitivity to the fault occurrence can be observed for the EKF algorithm. Significantly better results were obtained for ELO algorithm, and very small fault level – 1 or 2 shorted turns, can be detected easily with this algorithm (see also Fig. 7). Moreover, the calculation time for ELO is very short and fault indicator results are obtained on-line, in a real time.

6 CONCLUSION

The experimental tests proved the correctness of used theoretical models of the Extended Kalman Filter and the Extended Luenberger Observer, and demonstrated that the applied approach is suitable to the stator and rotor faults

detection of the inverter-fed induction motor.

Presented results show that both estimators present similar accuracy in case of the rotor faults, however the ELO algorithm is much simpler in practical realization and requires much less computational time.

In case of stator winding short circuits, the EKF presents smaller sensitivity to changeable number of shorten turns, especially in the incipient stator fault, compared to ELO. Moreover, in on-line diagnostics, it requires much more computational time, thus very fast digital processor is required.

The application of the EKF and ELO in the diagnostics based on mathematical modeling creates alternative to the classical, direct detection methods of the IM faults, based on the spectra analysis of the stator current and mechanical vibrations.

ACKNOWLEDGMENT

This research work was partly supported by the National Science Centre, Poland, under Grant NN510 637340 (2011-2013).

REFERENCES

[1] S. Bachir, S. Tani, J.-C. Trigeassou, G. Champenois, "Diagnosis by parameter estimation of stator and rotor faults occurring in induction machines", IEEE Trans. Ind. Electronics, vol. 53, no. 3, pp. 963-973, 2006.

[2] A.Bellini, F. Filippetti, C. Tassoni, G.A. Capolino, "Advances in Diagnostic Techniques for Induction Machines", IEEE Trans. Ind. Electron., vol.55, no.12, pp. 4109-4126, Dec. 2008

[3] C.H. De Angelo, G.R. Bossio, S.J. Giaccone, M.I. Valla, J.A. Solsona, G.O. Garcia, "On-line Model-Based Stator-Fault Detection and Identification in Induction Motors", IEEE Trans. Ind. Electron., vol.56, no.11, pp. 4671-4680, Nov. 2009

[4] M. Nait Said, M. Benbouzid, A. Benchaib, "Detection of Broken Bars in Induction Motors Using an Extended Kalman Filter for Rotor Resistance Sensorless Estimation", IEEE Trans. Energy Conversion, vol. 15, no. 1, pp. 66-70, March 2000.

[5] C. T. Kowalski, R. Wierzbicki, "Application of the extended Kalman filter for rotor and stator fault detection of the induction motor", Poznan Univ. Tech. Acad. Journal – El. Engineering, vol. 55, pp.154-157, 2007

[6] C. T. Kowalski, T. Orlowska-Kowalska, R. Wierzbicki, "Application of the State Estimators for Stator and Rotor Fault Monitoring of the Inverter-Fed Induction Motor Drive", 17th Int. Conf. on El. Drives and Power Electronics EDPE'2011, Slovak Rep., 2011, on CD

[7] T. Orlowska–Kowalska, "Sensorless induction motor drives", Wroclaw University of Technology Press, Wroclaw, Poland, 2003 (in Polish)

[8] H. Kubota, K. Matsuse, and T. Nakano, "DSP-based speed adaptive flux observer of induction motor", IEEE Trans. Ind. Appl., vol. 29, np.2, pp.344-348, March/Apr., 1993

Czeslaw T. Kowalski received his scientific degrees from Wroclaw University of Technology, Wroclaw, Poland, in 1971, 1983, 2006, respectively. He has the Professor position at Electrical Engineering Faculty of Wroclaw University of Technology, in the Electrical Drives, Mechatronics and Industrial Automation Chair of the Institute of Electrical Machines, Drives and Measurements. He is author and co-author of more than 150 journal papers and conference proceedings, two textbooks, one book. His field of interest is mathematical modeling and microprocessor control of electrical drives and power converters, monitoring and diagnosis of the electrical drives using state observers and neural networks.

Robert Wierzbicki received the MSc and PhD degrees from the Electrical Engineering Faculty, Wroclaw University of Technology, Wroclaw, Poland, in 2006 and 2011, respectively. He is an author and co-author of close to 20 scientific papers. His main fields of interest are the induction motor drive control and state variable estimation, and its application for diagnostic problems of AC electrical drives. Currently he is employed in Whirpool Poland in Wroclaw.

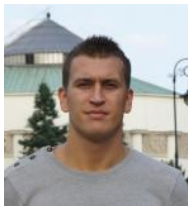

Marcin Wolkiewicz received the MSc and PhD degrees from the Electrical Engineering Faculty, Wroclaw University of Technology, Wroclaw, Poland, in 2007 and 2012, respectively. He has the Assistant Professor position at Electrical Engineering Faculty of Wroclaw University of Technology, in the Electrical Drives, Mechatronics and Industrial Automation Chair of the Institute of Electrical Machines, Drives and Measurements. He is an author and co-author of close to 30 scientific papers. His main fields of interest is monitoring and diagnosis of the electrical drives using signal analysis including advanced methods and transforms.

AUTHORS' ADDRESSES

Prof. Czeslaw T. Kowalski, Ph.D., D.Sc.
Wroclaw University of Technology
Institute of Electrical Machines, Drives and Measurements
ul. Smoluchowskiego 19, Wroclaw 50-372, Poland
email: czeslaw.t.kowalski@pwr.wroc.pl

Robert Wierzbicki, Ph.D.
Whirpool, Wroclaw, Poland
email: robert.wierzbicki@pwr.wroc.pl

Marcin Wolkiewicz , Ph.D.
Wroclaw University of Technology
Institute of Electrical Machines, Drives and Measurements
ul. Smoluchowskiego 19, Wroclaw 50-372, Poland
email: marcin.wolkiewicz @ pwr.wroc.pl

Received: 2012-01-15
Accepted: 2013-03-28